Characteristics of electromagnetic waves in slab waveguide structures comprising chiral nihility film and left-handed material claddings

Article *in* Optik - International Journal for Light and Electron Optics · September 2017

DOI: 10.1016/j.ijleo.2017.09.076

CITATIONS
0

READS
26

3 authors, including:

Khitam Elwasife
Islamic University of Gaza
29 PUBLICATIONS **79** CITATIONS

SEE PROFILE

Sofyan Taya
Islamic University of Gaza
150 PUBLICATIONS **1,134** CITATIONS

SEE PROFILE

Optik 149 (2017) 332–343

Contents lists available at ScienceDirect

Optik

journal homepage: www.elsevier.de/ijleo

Original research article

Characteristics of electromagnetic waves in slab waveguide structures comprising chiral nihility film and left-handed material claddings

Alaa N. Abu Helal, Khitam Y. Elwasife, Sofyan A. Taya *

Physics Department, Islamic University of Gaza, Gaza, Palestine, Palestine

ARTICLE INFO

Article history:
Received 18 March 2017
Accepted 19 September 2017

Keywords:
Slab waveguides
Chiral materials
Left-handed materials

ABSTRACT

We analytically present the dispersion equation of an asymmetric three-layered chirowaveguides, in which the core and the claddings are different chiral materials. Then, we produce the dispersion equation for a symmetric three-layered chirowaveguides, in which the claddings chiral materials are the same, but different from the one in the core. After that, two modes of propagation through a chiral nihility core and left handed material (LHM) claddings waveguide are treated in details. The characteristic equations and the cut-off frequencies for both even and odd modes are derived. The electric field profiles are plotted and discussed. We show that each mode (odd and even) can be separated into right-handed and left-handed circularly polarized (RCP and LCP) modes. The results reveal that novel properties such as peculiar dispersion curves.

1. Introduction

Macroscopic parameters such as the index of refraction (n), permitivity (ε), and permeability (μ) are used to study the interaction of an electromagnetic wave with a material, where it is impossible to take each atom or electron into account. Most materials have positive permitivity and permeability and are called douple posittive materials [1]. On the other hand, Veselago, in 1968, investigated therotically double negative materials with simultaneausly negative permitivity and permeability [1]. The features of these materials made them reffered to as left-handed materials (LHMs) or also to as negative index materials (NIMs). Comparing with conventional dielectric materials, LHMs have some unique properties such as a negative refrative index, sub wavelength imaging, backward wave propagation, and reverse Doppler and Cherenkov effects [2–17]. However, these materials do not exist in nature normally. After thirty years, Pendry developed the concept of a perfect lens [18]. The concept to make LHMs is to treat permitivity and permeability separately. Pendry used thin wire structure (wire array) to produce negative permitivity and magnet-free split-ring resonator (SRR) structure to produce negative permeability [19,20]. The first experimentally LHM was released by Shelby et al. where negative refraction in the microwave region was confirmed [21]. In the visible region, recent publications showed that obtaining negative values of real parts of the permitivity and permeability becomes available, but achieving a negative index of refraction becomes quite difficult because of high values of imaginary parts of permittivity [22]. Since then, much attention of this kind of metamaterial

* Corresponding author.
E-mail address: staya@iugaza.edu.ps (S.A. Taya).

http://dx.doi.org/10.1016/j.ijleo.2017.09.076
0030-4026/

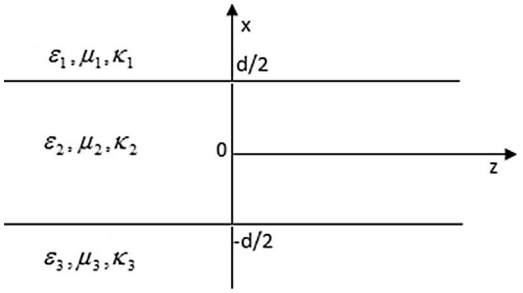

Fig. 1. Schemtaic digram of a waveguide consisting of three chiral medis.

has been drawn. LHMs have been proposed for many applications such as cloaking [23], micro strip patch antenna [24], wave absorbers [25] and biochemical sensos [26–34].

A long time ago, chiral materials were discovered and known as optical materials with high optical conductivity. The property of optical activity represents the ability to rotate the incident plane of a polarized wave. This rotation is attributed to the asymmetry in the molecular structure. These materials are characterized with a parameter known as the chirality parameter. When this parameter is larger than the index of refraction of the material at least near the resonant frequency, one eigen wave in the material becomes backward. As a result, the material becomes a negative-index material [35,36]. A polarized wave when entering a chiral bulk medium decomposed into two modes: right-handed circular polarization (RCP) and left-handed circular polarization (LCP). The velocities of the two waves differ from each other. When getting out from the chiral material, the two waves merge again and generate a linearly polarized wave. After leaving the chiral material, the linearly polarized wave makes an angle with the initial plane of polarization. The angle of rotation depends on many parameters such as the chiral medium thickness and the wavelength [37].

Due to the discovery of chiral media and its novel features, recent interest has been focused on the guided structures filled with chiral material, called'chirowaveguides [38–45]. Chirowaveguides, first suggested by p. pellet [38], have unique features that the propagation modes are hybrid since the electric and magnetic fields are coupled to each other by chirality.

In this paper, the propagation of s-polarized light (TE) in slab waveguides in which the core layer is chiral nihility material and the claddings are left-handed metamaterials is invetsiagted in details. The characteristic equations and field profile are derived and plotted. The energy guided by the wave is also investigated.

2. Theory

2.1. Dispersion equations of three-layered slab chiral waveguides

The geometry of an asymmetric slab chiral waveguide with thickness d is shown in Fig. 1. It consists of a thin chiral material film (permittivity ε_1, permeability μ_1 and chirality constant κ_1) bounded by isotropic chiral material upper and lower half spaces with different refractive index and chirality. Unlike the conventional dielectric materials, the electric and magnetic fields in chiral materials are coupled. This coupling is attributed to the chirality parameter and is expressed in the constitutive relations. Depending on which field vectors are used in the relations, the constitutive relations may take different, but equivalent, forms. The constitutive relations for the chiral media in this paper take the forms

$$D = \varepsilon_i E - j\kappa_i \sqrt{\varepsilon_0 \mu_0} H,\ B = \mu_i H + j\kappa_i \sqrt{\varepsilon_0 \mu_0} E \tag{1}$$

where ε_i and μ_i are the permitivity and permeability of medium i, respectively. κ_i is dimensionless and normalized quantity which represents the handedness of the medium, called the chirality. E, H, D and B are the electric, magnetic fields, electric displacement and magnetic flux density, respectively.

In chiral medium, electromagnetic fields are expressed as

$$E = E_+ + E_-, \quad H = H_+ + H_- \tag{2}$$

The electric and magnetic fields in chiral medium are related to each other by

$$H_\pm = \pm j.E_\pm/\eta_i \tag{3}$$

where the $(\pm)$ refter to right-handed and left-handed circularly polarized waves in the chiral medium, respectively, and $\eta_i = \sqrt{\mu_i/\varepsilon_i}$ is the wave impedance in the media. Substitution Eq. (2), and Eq. (3) into Maxwell's equations for source-free regions leads to the wave equations for RCP and LCP fields

$$\left(\nabla^2 + k_{i\pm}^2\right) E_\pm = 0 \tag{4}$$

where $k_{i\pm} = k_0(n_i \pm \kappa_i)$ is the effective index of refraction of both waves, $k_0 = \omega\sqrt{\varepsilon_0\mu_0}$ is the wave number in vaccum, and $n_i = \sqrt{\mu_i\varepsilon_i/\mu_0\varepsilon_0}$ is the refractive index of the chiral material. We consider the z dependence of the fields is $\exp\left(-j\beta z\right)$. The longitudinal field E_z can be written as

$$E_{z\pm}(x) = \begin{cases} A_{\pm} exp\left(-\gamma_{\pm}\left(x - \frac{d}{2}\right)\right), & x > d/2, \\ B_{\pm}\sin\left(\delta_{\pm}x\right), & -d/2 \le x \le d/2, \\ C_{\pm}\exp\left(\alpha_{\pm}\left(x + \frac{d}{2}\right)\right), & x < -d/2. \end{cases} \tag{5}$$

for odd guided modes, and

$$E_{z\pm}(x) = \begin{cases} A_{\pm} exp\left(-\gamma_{\pm}\left(x - \frac{d}{2}\right)\right), & x > d/2, \\ B_{\pm}\cos\left(\delta_{\pm}x\right), & -d/2 \le x \le d/2, \\ C_{\pm}\exp\left(\alpha_{\pm}\left(x + \frac{d}{2}\right)\right), & x < -d/2. \end{cases} \tag{6}$$

for even guided modes, where the parameters $\gamma_{\pm}$, $\delta_{\pm}$ and $\alpha_{\pm}$ are given by $\gamma_{\pm} = (\beta^2 - k_{1\pm}^2)^{1/2}$,$\delta_{\pm} = (k_{2\pm}^2 - \beta^2)^{1/2}$, $\alpha_{\pm} = (\beta^2 - k_{3\pm^2})^{1/2}$.

The other field components can be obtained by using Eqs. (2–4). According to the continuity requirement at the boundaries, the characteristic equations can be written as

$$\frac{4\gamma_+k_{2+}k_{2-}}{\delta_-}\left(\frac{\eta_2-\eta_1}{\eta_3}\right)\cos u_+\cos u_- + 4\left(\frac{\eta_2-\eta_1}{\eta_3}\right)(k_{1+}k_{2+})\sin u_-\cos u_+ +$$

$$\gamma_+k_{2+}\left(1+\frac{\eta_2}{\eta_3}\right)\left(1-\frac{\eta_2}{\eta_3}\right)\left(1+\frac{\eta_1}{\eta_2}\right)\left(\frac{k_{3-}}{\alpha_-}+\frac{k_{3+}}{\alpha_+}\right)\sin u_-\cos u_+ -$$

$$\left\{\frac{k_{3-}}{\alpha_-}(1-\frac{\eta_2}{\eta_3})^2+\frac{k_{3+}}{\alpha_+}(1+\frac{\eta_2}{\eta_3})^2\right\}\left(1-\frac{\eta_1}{\eta_2}\right)\left(\frac{\gamma_+\delta_+k_{2-}}{\delta_-}\right)\cos u_-\sin u_+ -$$

$$\left\{2\frac{k_{3-}}{\alpha_-}\left(1-\frac{\eta_2}{\eta_3}\right)\left(1+\frac{\eta_1}{\eta_3}\right)+2\frac{k_{3+}}{\alpha_+}\left(1+\frac{\eta_2}{\eta_3}\right)\left(1-\frac{\eta_1}{\eta_3}\right)\right\}\delta_+k_{1+}\sin u_+\sin u_- = 0 \tag{7}$$

for odd guided modes, and

$$\frac{-4\gamma_+k_{2+}k_{2-}}{\delta_-}\left(\frac{\eta_2-\eta_1}{\eta_3}\right)\sin u_+\sin u_- + 4\left(\frac{\eta_2-\eta_1}{\eta_3}\right)(k_{1+}k_{2+})\cos u_-\sin u_+ +$$

$$\gamma_+k_{2+}\left(1+\frac{\eta_2}{\eta_3}\right)\left(1-\frac{\eta_2}{\eta_3}\right)\left(1+\frac{\eta_1}{\eta_2}\right)\left(\frac{k_{3-}}{\alpha_-}+\frac{k_{3+}}{\alpha_+}\right)\cos u_-\sin u_+ -$$

$$\left\{\frac{k_{3-}}{\alpha_-}(1-\frac{\eta_2}{\eta_3})^2+\frac{k_{3+}}{\alpha_+}(1+\frac{\eta_2}{\eta_3})^2\right\}\left(1-\frac{\eta_1}{\eta_2}\right)\left(\frac{\gamma_+\delta_+k_{2-}}{\delta_-}\right)\sin u_-\cos u_+ +$$

$$\left\{2\frac{k_{3-}}{\alpha_-}\left(1-\frac{\eta_2}{\eta_3}\right)\left(1+\frac{\eta_1}{\eta_3}\right)+2\frac{k_{3+}}{\alpha_+}\left(1+\frac{\eta_2}{\eta_3}\right)\left(1-\frac{\eta_1}{\eta_3}\right)\right\}\delta_+k_{1+}\cos u_+\cos u_- = 0 \tag{8}$$

for even guided modes, where $u_{\pm} = \delta_{\pm}d/2$.

In the next we will study the dispersion equations of guided modes in a three-layered symmetric slab chiral waveguide.

If the chiral media in the claddings shown in Fig. 1 have the same refractive index and chirality as those of the substrate; $\kappa_1 = \kappa_3, \varepsilon_1 = \varepsilon_3$ and $\mu_1 = \mu_3$, then we have a symmetric three- layered slab chiral waveguide. The solutions of the longitudinal-field component in Eq. (4) are written as

$$E_{z\pm}(x) = \begin{cases} A_\pm \exp\left(-\gamma_\pm\left(x - \frac{d}{2}\right)\right), & x > d/2, \\ B_\pm \sin\left(\delta_\pm x\right), & -d/2 \le x \le d/2, \\ A_\pm \exp\left(\gamma_\pm\left(x + \frac{d}{2}\right)\right), & x < -d/2. \end{cases} \tag{9}$$

for odd guided modes, and

$$E_{z\pm}(x) = \begin{cases} A_\pm \exp\left(-\gamma_\pm\left(x - \frac{d}{2}\right)\right), & x \ge d/2, \\ B_\pm \cos\left(\delta_\pm x\right), & -d/2 < x < d/2, \\ A_\pm \exp\left(\gamma_\pm\left(x + \frac{d}{2}\right)\right), & x \le -d/2. \end{cases} \tag{10}$$

for even guided modes.

Other components of the fields are obtained and the continuity requirements are applied, we obtain the following dispersion relations

$$\frac{4k_{2+}k_{2-}}{\delta_+\delta_-}\cos u_+\cos u_- + \frac{4k_{1+}k_{1-}}{\gamma_+\gamma_-}\sin u_+\sin u_- - \left(\frac{1}{\eta_1\eta_2}\right)\left\{\left(\frac{k_{1+}k_{2+}}{\delta_+\gamma_+}(\eta_1-\eta_2)^2 + \frac{k_{1-}k_{2+}}{\delta_+\gamma_-}(\eta_1+\eta_2)^2\right)\sin u_-\cos u_+ + \left(\frac{k_{1-}k_{2-}}{\delta_-\gamma_-}(\eta_1-\eta_2)^2 + \frac{k_{1+}k_{2-}}{\delta_-\gamma_+}(\eta_1+\eta_2)^2\right)\cos u_-\sin u_+\right\} = 0 \tag{11}$$

for odd guided modes, and

$$\frac{4k_{1+}k_{1-}}{\gamma_+\gamma_-}\cos u_+\cos u_- + \frac{4k_{2+}k_{2-}}{\delta_+\delta_-}\sin u_+\sin u_- + \left(\frac{1}{\eta_1\eta_2}\right)\left\{\left(\frac{k_{1-}k_{2-}}{\delta_-\gamma_-}(\eta_1-\eta_2)^2 + \frac{k_{1+}k_{2-}}{\delta_-\gamma_+}(\eta_1+\eta_2)^2\right)\sin u_-\cos u_+ + \left(\frac{k_{1+}k_{2+}}{\delta_+\gamma_+}\right)(\eta_1-\eta_2)^2 + \frac{k_{1-}k_{2+}}{\delta_+\gamma_-}(\eta_1+\eta_2)^2\cos u_-\sin u_+\right\} = 0 \tag{12}$$

for even guided modes.

2.2. Dispersion equations of three-layered symmetric slab chiral core and achiral claddings waveguides

When the waveguide consists of a chiral core and an achiral claddings, where $\kappa_1 = 0$, the above parameters become $k_{1\pm} = n_1 k_0 = k_1$, $k_{2\pm} = k_0(n_2 \pm \kappa_2)$, $\gamma_\pm = (\beta^2 - k_1^2)^{1/2} = \gamma$, $\delta_\pm = (k_{2\pm}^2 - \beta^2)^{1/2}$.

The dispersion Eqs. (11), (12) reduce to

$$\frac{2k_0^2\left(n_2^2 - \kappa_2^2\right)}{\delta_+\delta_-}\cos u_+\cos u_- + \frac{2k_1^2}{\gamma^2}\sin u_+\sin u_- - \frac{k_1\left(\eta_1^2+\eta_2^2\right)}{\gamma\eta_1\eta_2}\left\{\left(\frac{k_{2+}}{\delta_+}\right)\sin u_-\cos u_+ + \left(\frac{k_{2-}}{\delta_-}\right)\cos u_-\sin u_+\right\} = 0 \tag{13}$$

for odd guided modes, and

$$\frac{2k_1^2}{\gamma^2}\cos u_+\cos u_- + \frac{2k_0^2\left(n_2^2 - \kappa_2^2\right)}{\delta_+\delta_-}\sin u_+\sin u_- + \frac{k_1\left(\eta_1^2+\eta_2^2\right)}{\gamma\eta_1\eta_2}\left\{\left(\frac{k_{2+}}{\delta_+}\right)\cos u_-\sin u_+ + \left(\frac{k_{2-}}{\delta_-}\right)\sin u_-\cos u_+\right\} = 0 \tag{14}$$

for even guided modes.When the guiding layer is chiral nihility with a permittivity and permeability of zero value, the above parameters become $k_{1\pm} = n_1 k_0 = k_1$, $k_{2\pm} = \pm k_0\kappa_2$, $\gamma_\pm = (\beta^2 - k_1^2)^{1/2} = \gamma$, $\delta_\pm = (k_{2\pm}^2 - \beta^2)^{1/2} = (k_0^2\kappa_2^2 - \beta^2)^{1/2} = \delta$

The dispersion relation given by Eq. (13) can be divided into two equations as

$$(k_0^2\kappa_2^2 - \beta^2)^{\frac{1}{2}}\frac{d}{2} = tan^{-1}\{\frac{k_0\kappa_2}{k_1}(\frac{\beta^2 - k_1^2}{k_0^2\kappa_2^2 - \beta^2})^{\frac{1}{2}}\} + m\pi, m = 0, 1, 2, . \tag{15}$$

for RCP odd modes, and

$$(k_0^2\kappa_2^2 - \beta^2)^{\frac{1}{2}}\frac{d}{2} = -tan^{-1}\left\{\frac{k_0\kappa_2}{k_1}\left(\frac{\beta^2 - k_1^2}{k_0^2\kappa_2^2 - \beta^2}\right)^{1/2}\right\} + m\pi, m = 1, 2, 3, . \tag{16}$$

for LCP odd modes, where m is mode number. It is noted that m starts from 0 in RCP odd modes and from 1 in LCP odd modes.

Moreover, the dispersion relation given by Eq. (14) can also be divided into two equations, taking in mind that RCP and LCP even guided modes are mirror images of RCP and LCP odd guided modes, then the dispersion equations take the form

$$(k_0^2\kappa_2^2-\beta^2)^{\frac{1}{2}}\frac{d}{2}=-tan^{-1}\{\frac{k_1}{k_0\kappa_2}(\frac{k_0^2\kappa_2^2-\beta^2}{\beta^2-k_1^2})^{\frac{1}{2}}\}+m\pi,\ m=1,2,3,. \tag{17}$$

for RCP even modes, and

$$(k_0^2\kappa_2^2-\beta^2)^{\frac{1}{2}}\frac{d}{2}=tan^{-1}\{\frac{k_1}{k_0\kappa_2}(\frac{k_0^2\kappa_2^2-\beta^2}{\beta^2-k_1^2})^{\frac{1}{2}}\}+m\pi,\ m=0,1,2,. \tag{18}$$

for LCP even modes. As can be seen, m starts from 1 in RCP even modes and from 0 in LCP even modes, because of the handedness of chiral meta-material. This is in contray to odd modes.

2.3. Guided modes in slab chiral nihility core and LHM claddings waveguides

We assume chiral nihility core and the claddings are left-handed materials. It is shown that the dispersion relation given by Eq. (13) and Eq. (14) can be splitted into two different dispersion relation corresponding to RCP and LCP modes, respectively. For the two cases of odd and even modes, we present the characteristic equation and the cut-off frequency. Moreover, the field profile and the energy guided by the wave of RCP and LCP modes are also presnented.

2.3.1. Odd modes

We use in the claddings left-handed materials (LHMs), which, by definition, have a negative refractive index. The parameter n_1 have a negative value, so the dispersion relation given by Eq. (13) is divided into two equations as

$$(k_0^2\kappa_2^2-\beta^2)^{\frac{1}{2}}\frac{d}{2}=tan^{-1}\{\frac{k_0\kappa_2}{k_1}(\frac{\beta^2-k_1^2}{k_0^2\kappa_2^2-\beta^2})^{\frac{1}{2}}\}+m\pi,\ m=1,2,3,. \tag{19}$$

for RCP odd modes, and

$$(k_0^2\kappa_2^2-\beta^2)^{\frac{1}{2}}\frac{d}{2}=-tan^{-1}\{\frac{k_0\kappa_2}{k_1}(\frac{\beta^2-k_1^2}{k_0^2\kappa_2^2-\beta^2})^{\frac{1}{2}}\}+m\pi,\ m=0,1,2. \tag{20}$$

for LCP odd modes. As can be seen m starts from 0 in LCP odd modes and from 1 in RCP odd modes. This is in contadiction of Eqs. (15) and (16).

We can obtain the normalized cutoff frequencies (V) by setting $\beta\rightarrow\kappa_1$ in the dispersion Eqs. (19) and (20)

$$V=k_0d=\frac{2m\pi}{(\kappa_2^2-n_1^2)^{1/2}},\ m=1,2,3,. \tag{21}$$

for RCP odd modes, and

$$V=k_0d=\frac{2m\pi}{(\kappa_2^2-n_1^2)^{1/2}},\ m=0,1,2,. \tag{22}$$

for LCP odd modes.

We can express the electromagnetic fields in explicit forms as

$$E_x(x)=\begin{cases}-\frac{j\beta A}{\gamma}\exp\left\{-\gamma\left(x-\frac{d}{2}\right)\right\} & \mathrm{x}>d/2,\\ -\frac{j\beta A}{\delta\sin(u)}\cos\left(\delta x\right) & -\mathrm{d}/2\le\mathrm{x}\le\mathrm{d}/2,\\ +\frac{j\beta A}{\gamma}\exp\left\{\gamma\left(x+\frac{d}{2}\right)\right\} & \mathrm{x}<-d/2.\end{cases} \tag{23}$$

$$E_y(x) = \begin{cases} \mp\dfrac{k_1 A}{\gamma}\exp\left\{-\gamma\left(x-\dfrac{d}{2}\right)\right\} & \mathrm{x} > d/2, \\ -\dfrac{k_0\kappa_2 A}{\delta\sin(u)}\cos\left(\delta x\right) & -\mathrm{d}/2 \le \mathrm{x} \le \mathrm{d}/2, \\ \pm\dfrac{k_1 A}{\gamma}\exp\left\{\gamma\left(x+\dfrac{d}{2}\right)\right\} & \mathrm{x} < -d/2. \end{cases} \tag{24}$$

and

$$E_z(x) = \begin{cases} A exp\left\{-\gamma\left(x-d/2\right)\right\} & \mathrm{x} > d/2, \\ \dfrac{A}{\sin(u)}\sin\left(\delta x\right) & -\mathrm{d}/2 \le \mathrm{x} \le \mathrm{d}/2, \\ A\exp\left\{\gamma\left(x+d/2\right)\right\} & \mathrm{x} < -d/2. \end{cases} \tag{25}$$

for RCP (upper sign) and LCP (lower sign) odd modes, respectively. A is a constant and can be determined from the power flow.

The magnetic fields are determined from the well-known equation

$$H_{x,y,z} = \pm\frac{j}{\eta_1}E_{x,y,z} \tag{26}$$

for RCP (upper sign) and LCP (lower sign) odd modes, respectively.

The energy flowing in the waveguide is detemined from Poynting vector as

$$S_z = \frac{1}{2}Re(E\times H^*) = \frac{1}{2}Re\left(E_x H_y^* - E_y H_x^*\right) \tag{27}$$

Thus we can express enery flow along the z-axis as

$$S_z(x) = \begin{cases} \dfrac{\beta k_1 A^2}{\eta_1\gamma^2}exp\left\{-2\gamma\left(x-\dfrac{d}{2}\right)\right\} & \mathrm{x} > d/2, \\ \pm\dfrac{\beta k_0\kappa_2 A^2}{\eta_1\delta^2\sin^2(u)}\cos^2\left(\delta x\right) & -\mathrm{d}/2 \le \mathrm{x} \le \mathrm{d}/2, \\ \dfrac{\beta k_1 A^2}{\eta_1\gamma^2}\exp\left\{2\gamma\left(x+\dfrac{d}{2}\right)\right\} & \mathrm{x} < -d/2. \end{cases} \tag{28}$$

for RCP (upper sign) and LCP (lower sign) odd modes, respectively. As can be seen from Eq. (28), the z-compnenet of S is positive for RCP odd modes and negative for LCP odd modes in the core, and positive for both RCP and LCP odd modes in the claddings. On the other hand, we use LHM claddings which make the energy flux negative in the claddings for both RCP and LCP odd modes.

2.3.2. Even modes

When the claddings are left-handed materials (LHMs) and the index n_1 have a negative value, the dispersion relation (Eq. (14)) can be divided into two equations as

$$(k_0^2\kappa_2^2-\beta^2)^{\frac{1}{2}}\frac{d}{2} = -tan^{-1}\{\frac{k_1}{k_0\kappa_2}(\frac{k_0^2\kappa_2^2-\beta^2}{\beta^2-k_1^2})^{\frac{1}{2}}\} + m\pi, m = 0, 1, 2, . \tag{29}$$

for RCP even modes, and

$$(k_0^2\kappa_2^2-\beta^2)^{\frac{1}{2}}\frac{d}{2} = tan^{-1}\{\frac{k_1}{k_0\kappa_2}(\frac{k_0^2\kappa_2^2-\beta^2}{\beta^2-k_1^2})^{\frac{1}{2}}\} + m\pi, m = 1, 2, 3, . \tag{30}$$

for LCP even modes.

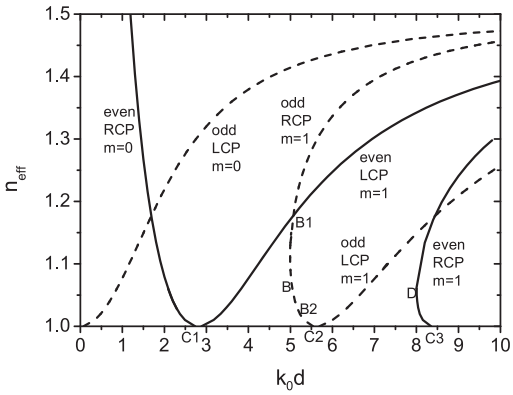

Fig. 2. The dispersion curves for the first few modes.

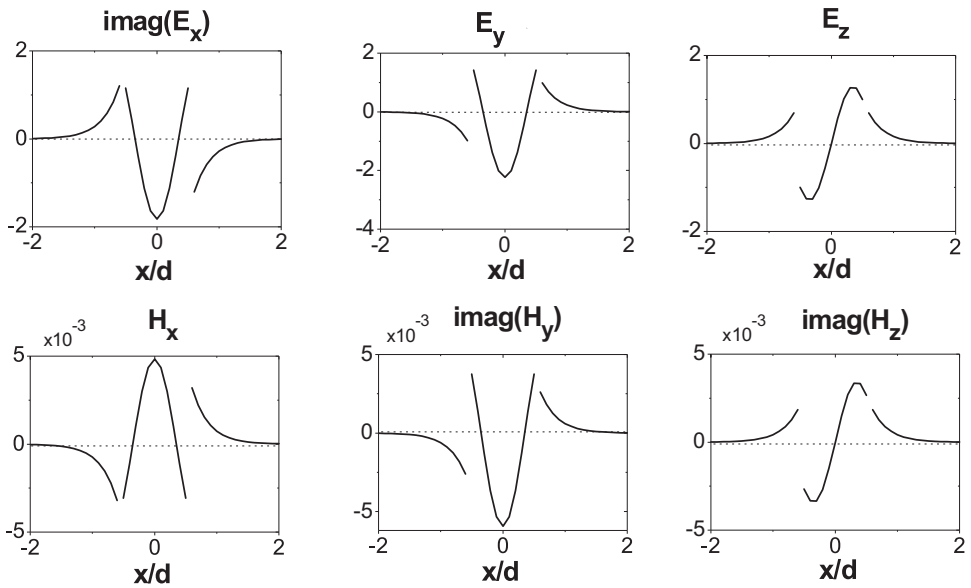

Fig. 3. The electric and magnetic field components $k_0d = 5.2$ for RCP odd mode when m = 1,n_{eff} = 1.223.

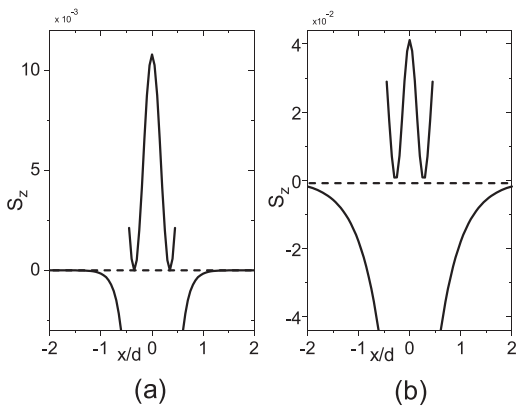

Fig. 4. Energy flux at $k_0d = 5.2$ for RCP odd mode when m = 1, (a) n_{eff} = 1.223; (b) n_{eff} = 1.02219.

The normalized cutoff frequencies is abtained by setting $\beta \to \kappa_1$ in the dispersion Eqs. (29) and (30)

$$V = k_0 d = \frac{(2m+1)\pi}{(\kappa_2^2 - n_1^2)^{1/2}}, m = 0, 1, 2, . \tag{31}$$

for RCP even modes, and

$$V = k_0 d = \frac{(2m-1)\pi}{(\kappa_2^2 - n_1^2)^{1/2}}, m = 1, 2, 3, . \tag{32}$$

for LCP even modes.

We can express the electromagnetic fields in explicit forms as

$$E_x(x) = \begin{cases} -\dfrac{j\beta A}{\gamma} exp\left\{-\gamma\left(x - \dfrac{d}{2}\right)\right\} & x > d/2, \\ +\dfrac{j\beta A}{\delta \cos(u)} \sin(\delta x) & -d/2 \le x \le d/2, \\ +\dfrac{j\beta A}{\gamma} \exp\left\{\gamma\left(x + \dfrac{d}{2}\right)\right\} & x < -d/2. \end{cases} \tag{33}$$

$$E_y(x) = \begin{cases} \mp\dfrac{k_1 A}{\gamma} exp\left\{-\gamma\left(x - \dfrac{d}{2}\right)\right\} & x > d/2, \\ +\dfrac{k_0 \kappa_2 A}{\delta \cos(u)} \sin(\delta x) & -d/2 \le x \le d/2, \\ \pm\dfrac{k_1 A}{\gamma} \exp\left\{\gamma\left(x + \dfrac{d}{2}\right)\right\} & x < -d/2. \end{cases} \tag{34}$$

and

$$E_z(x) = \begin{cases} A exp\left\{-\gamma\left(x - \dfrac{d}{2}\right)\right\} & x > d/2, \\ \dfrac{A}{\cos(u)} \cos(\delta x) & -d/2 \le x \le d/2, \\ A \exp\left\{\gamma\left(x + \dfrac{d}{2}\right)\right\} & x < -d/2. \end{cases} \tag{35}$$

for RCP (upper sign) and LCP (lower sign) even modes, respectively.

The magnetic fields in the core and the claddings are given by Eq. (26). We can express the enery flow along the z-axis in the waveguide as

$$S_z(x) = \begin{cases} \dfrac{\beta k_1 A^2}{\eta_1 \gamma^2} exp\left\{-2\gamma\left(x - \dfrac{d}{2}\right)\right\} & x > d/2, \\ \pm\dfrac{\beta k_0 \kappa_2 A^2}{\eta_1 \delta^2 \cos^2(u)} \sin^2(\delta x) & -d/2 \le x \le d/2, \\ \dfrac{\beta k_1 A^2}{\eta_1 \gamma^2} \exp\left\{2\gamma\left(x + \dfrac{d}{2}\right)\right\} & x < -d/2. \end{cases} \tag{36}$$

for RCP (upper sign) and LCP (lower sign) even modes, respectively. Also, it is obvious from Eq. (36) that S_z is positive for RCP even modes and negative for LCP even modes in the core, and positive for both RCP and LCP even modes in the claddings. On the other hand, we use LHM claddings which make the energy flux negative in the claddings for both RCP and LCP even modes.

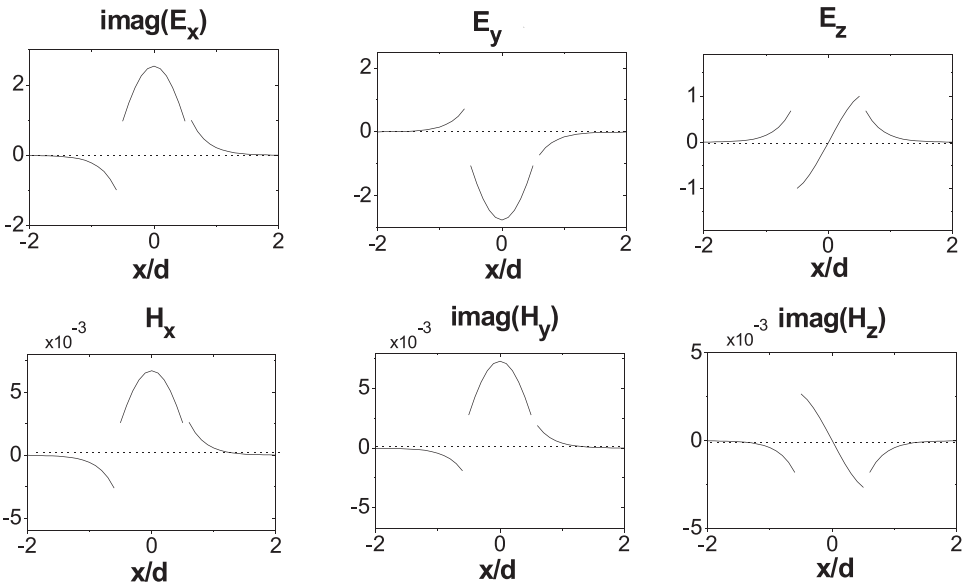

Fig. 5. Amplitudes of electromagnetic field components at $k_0d = 4$ for LCP odd mode when m = 0.

3. Results and discussion

We can calculate the propagation constants numerically from the dispersion eqs. (19), (20), (29), (30), then the electromagnetic fields and the energy flow distribution can be calculated. In this section, we assume chiral nihility core guiding film with the parameters $\mu_2 = \varepsilon_2 = 0$, $\kappa_2 = 1.5$. On the other hand, the cladding and substrate are LHMs with parameters$\mu_1 = (-1 + .001\mathrm{i}) \times \mu_0$, $\varepsilon_1 = (-1 + .001\mathrm{i}) \times \varepsilon_0$, and $\kappa_1 = 0$.

3.1. Dispersion curves

The dispersion curves are very important for understanding the wave propagation in slab waveguide structures. For the low-order modes, we show in Fig. 2 the dispersion curves in the slab chiral nihility core and LHMs claddings waveguide. The figure shows the dispersion curves of both odd and even guided modes. The y-axis represent n_{eff} where n_{eff} is the effective refractive index and is given by $n_{eff} = \beta/k_0$. The horizontal axis represents k_0d, where k_0d is the normalized frequency. The solid curves represent even modes whereas dashed curves represent odd modes. As can be seen from the figure, the dispersion curves of LCP odd and even modes increases monotonically with the increase of k_0d. The figure reveals that the cut-off frequencies (points C_1, C_2) satisfy Eq. (22) or Eq. (32). On the other hand, in the RCP odd and even modes, the characteristic curves are no longer increasing monotonically. They are bent so that the cut-off frequencies are not the minimum frequencies that waves can propagate. For example, consider the fundamental mode (m = 0), there is one solution below cut-off frequency (point C_1) for RCP even mode. If the consider the first guided mode (m = 1), there are two solutions below cut-off frequency (points C_2, C_3) for both RCP even and odd modes. This behavior of the dispersion curves reveals peculiar dispersion curves. In these cases, the cut-off frequency is not actually "cut-off" since the actual cut-off is the minimum frequency (critical points B, D) at which guided wave can propagate. As the frequency increases from the critical points B, D the dispersion curves split into two divisions. The two subdivisions are chrarateriszed by increasing the effective refractive index (upper division) and decreasing the effective index (lower division).

3.2. Odd guided modes

Figs. 3 and 4 illustrate the electric and magnetic field components and the z-component of the Poynting vector at the value of $k_0d = 5.2$ for RCP odd mode for the first guided mode (m = 1). E_z and H_z are odd functions of x (sin form) and E_x, E_y, H_x, and H_y (cos form) are even functions of x. S_z is positive in the core and is negative in the claddings due to the negative refractive index of LHM claddings. However, there are two propagation constants at $k_0d = 5.2$.

The electric and magnetic field components and the z-component of the Poynting vector are plotted in Figs. 5 and 6 at the value $k_0d = 4$ for LCP odd mode when m = 0. E_z, H_z are odd functions of x (sin form) and E_x, E_y, H_x, H_y (cos form) are even functions of x. The z-component of the Poynting vector is negative in both the core and the claddings.

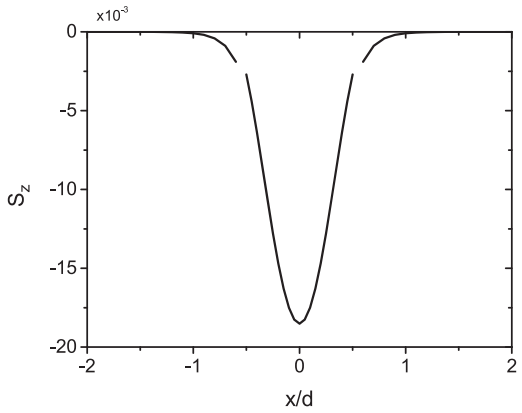

Fig. 6. Energy flux at $k_0d = 4$ for LCP odd mode when m = 0.

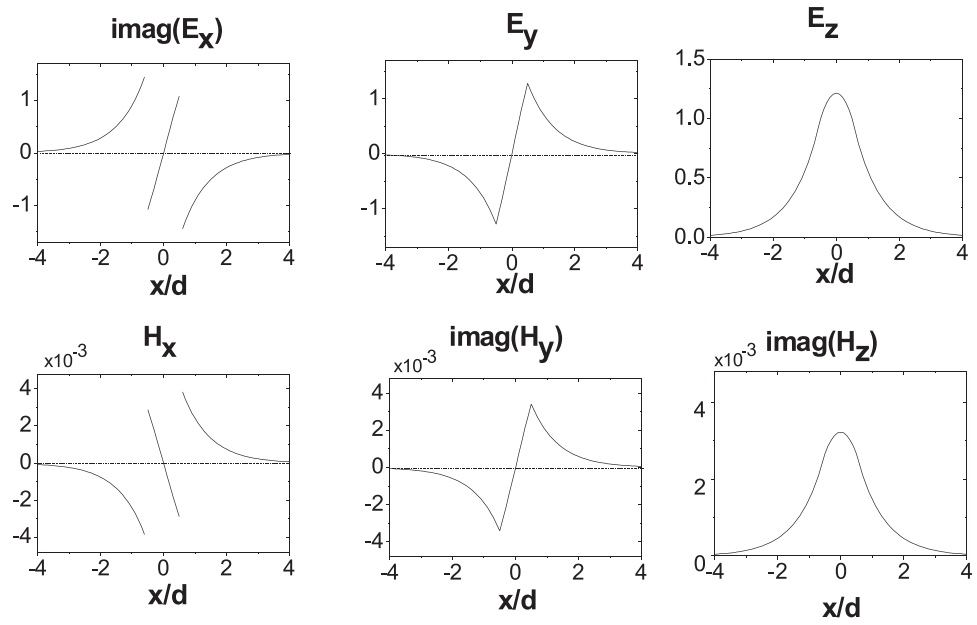

Fig. 7. Amplitudes of electromagnetic field components at $k_0d = 1.5$ for RCP even mode when m = 0.

3.3. Even guided modes

Figs. 7 and 8 illustrate the electric and magnetic field components and the z-component of the Poynting vector at the value $k_0d = 1.5$ for RCP even mode when m=0. E_z, H_z are even functions of x (cos form) and E_x, E_y, H_x, H_y (sin form) are odd functions of x. S_z is positive in the core and is negative the claddings due to the negative refractive index of LHM claddings.

The electric and magnetic field components and the z-component of the Poynting vector are plotted in Figs. 9 and 10 at the value $k_0d = 6$ for LCP even mode when m=1. E_z, H_z are even functions of x (cos form) and E_x, E_y, H_x, H_y (sin form) are odd functions of x. S_z is negative in both the core and the claddings (due to the negative refractive index of LHM claddings).

4. Conclusion

Dispersion relations of three-layered asymmetric and symmetric chiral slab waveguides were presented. We first considered all the layers constituting the waveguide are chiral. We then take the special case of slab chiral nihility core and LHMs claddings. The characteristic equations for odd and even guided modes were derived. It was found that each of these modes can be classified into right-handed and left-handed circularly polarized (RCP and LCP) modes. In each case of the odd and even modes, we presented the characteristic equations and the longitudinal component of the Poynting vector. Moreover, both the cut-off frequencies and the field profiles were also presented, plotted and discussed. Numerical results for

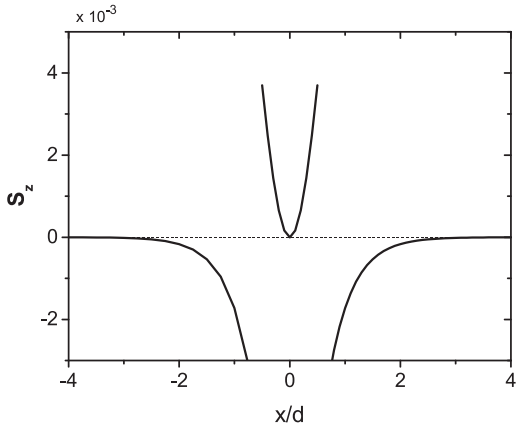

Fig. 8. Energy flux at $k_0d = 1.5$ for RCP even mode when m = 0.

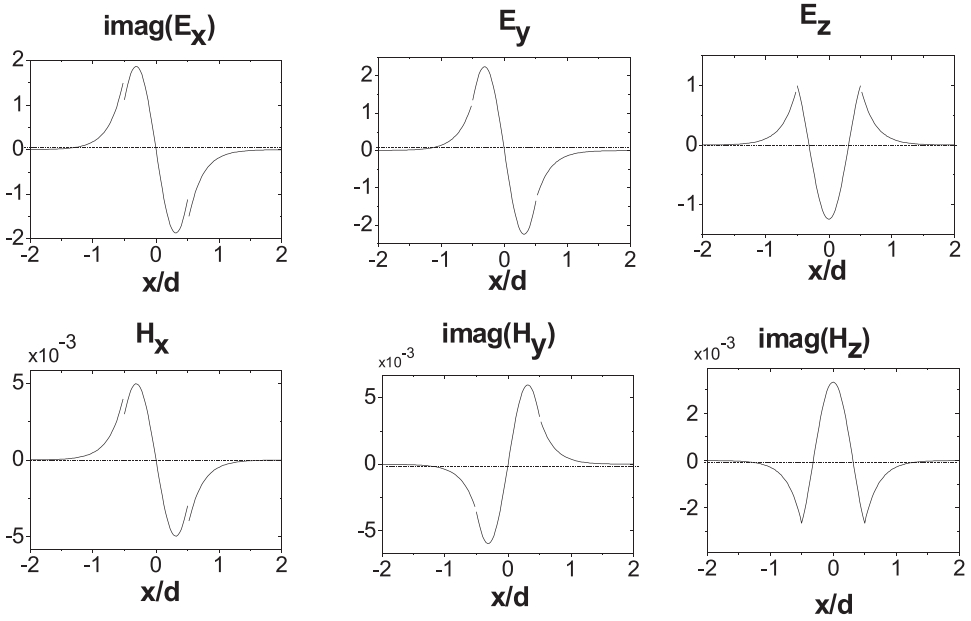

Fig. 9. Amplitudes of electromagnetic field components at $k_0d = 6$ for LCP even mode when m = 1.

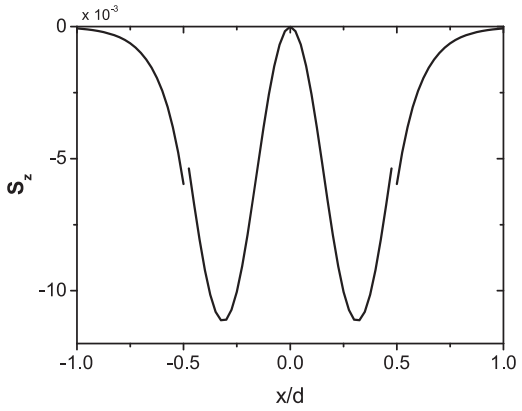

Fig. 10. Energy flux at $k_0d = 6$ for LCP even mode when m = 1.

typical chirality parameters of several low-order guided modes were provided. Some unusual properties such as abnormal dispersion curves in the chiral nihility waveguides were found.

References

[1] V.G. Veselago, The electrodynamics of substances with simultaneously negative values of ε and μ, Sov. Phy. Usp. 10 (1968) 509–514.
[2] H. Chen, B.-I. Wu, J.A. Kong, Review of electromagnetic theory in left-handed materials, J. Electromagn. Waves Appl. 20 (2006) 2137–2151.
[3] C.-W. Qiu, N. Burokur, S. Zouhd, Le-Wei Li, Chiral nihility effects on energy flow in chiral materials, J. Opt. Soc. Am. A 25 (2008) 55–63.
[4] S.A. Taya, E.J. El-Farram, M.M. Abadla, Symmetric multilayer slab waveguide structure with a negative index material: TM case, Optik – Int. J. Light Electron Opt. 123 (2012) 2264–2268.
[5] S.A. Taya, I.M. Qadoura, Guided modes in slab waveguides with negative index cladding and substrate, Optik – Int. J. Light Electron Opt. 124 (2013) 1431–1436.
[6] S.A. Taya, K.Y. Elwasife, Guided modes in a metal-clad waveguide comprising a left-handed material as a guiding layer, Int. J. Res. Rev. Appl. Sci. (IJRRAS) 13 (2012) 294–305.
[7] I.M. Qadoura, S.A. Taya, K.Y. El-wasife, Scaling rules for a slab waveguide structure comprising nonlinear and negative index materials, Int. J. Microw. Opt. Technol. (IJMOT) 7 (2012) 349–357.
[8] V.I. Shadrivov, Nonlinear guided waves and symmetry breaking in left-handed waveguides, Photonics and Nanostruct. – Fundam. Appl. 2 (2004) 175–180.
[9] M.A. Abadla, S.A. Taya, Characteristics of left-handed multilayer slab waveguide structure, The Islamic University Journal (Series of Natural Studies and Engineering) 19 (2011) 57–70.
[10] S.A. Taya, H.M. Kullab, Ibrahim M. Qadoura, Dispersion properties of slab waveguides with double negative material guiding layer and nonlinear substrate, J. Opt. Soc. Am. B 30 (2013) 2008–2013.
[11] Z. Wang, S. Li, Quasi-optics of the surface guided modes in a left-handed material slab waveguide, J. Opt. Soc. Am. 25 (2008) 903–908 (B).
[12] S.A. Taya, K.Y. Elwasife, H.M. Kullab, Dispersion properties of anisotropic-metamaterial slab waveguide structure, Opt. Appl. 43 (2013) 857–869.
[13] M. Abadla, S.A. Taya, Excitation of TE surface polaritons in different structures comprising a left-handed material and a metal, Optik – Int. J. Light Electron Opt. 125 (2014) 1401–1405.
[14] S.A. Taya, K.Y. Elwasife, Field profile of asymmetric slab waveguide structure with LHM layers, J. Nano- Electron. Phys. 6 (2014) 02007–02011.
[15] S.A. Taya, Dispersion properties of lossy, dispersive, and anisotropic left-handed material slab waveguide, Optik – Int. J. Light Electron Opt. 126 (2015) 1319–1323.
[16] S.A. Taya, D.M. Alamassi, Reflection and transmission from left-handed material structures using Lorentz and Drude medium models, Opto-Electron. Rev. 23 (2015) 214–221.
[17] T. Koschny, R. Moussa, C. Soukoulis, Limits on the amplification of evanescent waves of left-handed materials, J. Opt. Soc. Am. 23 (2006) 485–489 (B).
[18] J.B. Pendry, Negative refraction makes a perfect lens, Phys. Rev 85 (2000) 3966–3969.
[19] J.B. Pendry, A.J. Holden, D.J. Robbins, W.J. Stewart, Low frequency plasmons in thin-wire structures, Phys. Condens. Matter 10 (1998) 4785–4809.
[20] J.B. Pendry, A.J. Holden, D.J. Robbins, W.J. Stewart, Magnetism from conductors and enhanced nonlinear phenomena, IEEE Tran. Micr. Theo. Tech. 47 (1999) 2075–2084.
[21] R.A. Shelby, D.R. Smith, S. Schultz, Experimental verification of a negative index of refraction, Science 292 (2001) 77–79.
[22] N. Grigorenko, A.K. Geim, H.F. Gleeson, Y. Zhang, A.A. Firsov, I.Y. Khrushchev, J. Petrovic, Nanofabricated media with negative permeability at visible frequencies, Nature 438 (2005) 335–338.
[23] T. Ergin, N. Stenger, P. Brenner, J.B. Pendry, M. Wegener, Three-dimensional invisibility cloak at optical wavelengths, Sci. J. 328 (2010) 337–339.
[24] L.W. Li, Y.N. Li, T.S. Yeo, J.R. Mosig, O.J. Martin, A broadband and high-gain metamaterial microstrip antenna, Appl. Phys. Lett. 96 (2010) 164–165.
[25] Zh. Zhang, Zh. Wang, L. Wang, Design principle of single- or double-layer wave-absorbers containing left-handed materials, Mater. Des. 30 (2009) 3908–3912.
[26] H.M. Kullab, S.A. Taya, T.M. El-Agez, Metal-clad waveguide sensor using a left-handed material as a core layer, J. Opt. Soc. Am. B 29 (2012) 959–964.
[27] H.M. Kullab, S.A. Taya, Peak type metal-clad waveguide sensor using negative index materials, Int. J. Electron. Commun. (AEÜ) 67 (2013) 905–992.
[28] H.M. Kullab, S.A. Taya, Transverse magnetic peak type metal-clad optical waveguide sensor, Optik – Int. J. Light Electron Opt. 145 (2014) 97–100.
[29] S.A. Taya, H.M. Kullab, Optimization of transverse electric peak type metal-clad waveguide sensor using double negative materials, Appl. Phys. A 116 (2014) 1841–1846.
[30] S.A. Taya, Slab waveguide with a.ir core layer and anisotropic left-handed material claddings as a sensor, Opto-Electron. Rev. 22 (2014) 252–257.
[31] S.A. Taya, P-polarized surface waves in a slab waveguide with left-handed material for sensing applications, J. Magn. Magn.Mater. 377 (2015) 281–285.
[32] S.A. Taya, Theoretical investigation of slab waveguide sensor using anisotropic metamaterials, Optica Appl. 45 (2015) 405–417.
[33] H.M. Kullab, I.M. Qadoura, S.A. Taya, Slab waveguide sensor with left-handed material core layer for detection an adlayer thickness and index, J. Nano- Electron. Phys. 7 (2015) 02039–02044.
[34] S.A. Taya, A.A. Jarada, H.M. Kullab, Slab waveguide sensor utilizing left-handed material core and substrate layers, Optik – Int. J. Light Electron Opt. 127 (2016) 7732–7739.
[35] J. Dong, C. Xu, Characteristics of guided modes in planner chiral nihility meta-material waveguides, Prog. Electromagn. Res. B 14 (2009) 107–126.
[36] C. Zhang, T.J. Cui, Negative reflections of electromagnetic waves in chiral media, Appl. Phys. Lett. 91 (2007).
[37] A. Elsherbeni, V. Demir, E. Al Sharkawy, S. Arvas, Electromagnetic Scattering From Chiral Media, Progress in Electromagnetic Research Symposium, Pisa, Italy, March 28–31, 2004, pp. 799–802.
[38] P. Pelet, N. Engheta, The theory of chirowaveguides, IEEE Trans. Antennas and Propag. 38 (1990) 90–98.
[39] M. Oksanen, P.K. Kolivisto, I.V. lindell, Dispersion curves and fields for a chiral slab waveguide, IEEE Proc. -H 138 (1991) 327–344.
[40] C. Caloz, C. Chang, T. Itoh, Full-wave verification of the fundamental properties of left-handed materials in waveguide configurations, J. Appl. Phys. 90 (2001) 5483–5486.
[41] J. Xiao, K. Zhang, L. Gong, Field analysis of a general chiral planer waveguide, Int. J. Infrared and Millim. Waves 18 (1997) 939–948.
[42] Z.J. Wang, J.F. Dong, Analysis of guided modes in asymmetric left-handed slab waveguides, Prog. Electromagn. Res. 62 (2006) 203–215.
[43] D.R. Smith, N. Kroll, Negative refractive index in left-Handed materials, Phys. Rev. Lett. 85 (2000) 2933–2936.
[44] M. Yokota, Y. Yamanaka, Dispersion relation and field distribution for a chiral slab waveguide, Int. J. Microw. Optic. Technol. 1 (2006) 623–627.
[45] J.F. Dong, J. Li, Characteristics of guided modes in uniaxial chiral circular waveguides, Prog. Electromagn. Res. 124 (2012) 331–345.